_____

PHOTOCATALYTIC FORMATION AND PHOTOINDUCED CHARGING OF ZnO–Au NANOSTRUCTURES

O.L. Stroyuk[1*], **V.V. Shvalagin**[1], **I.E. Kotenko**[1], **S.Ya. Kuchmiy**[1], **A.G. Derzhypolskiy**[2,3],
D.A. Melenevskiy[2,3]

[1]*Pysarzhevskiy Institute of Physical Chemistry of National Academy of Sciences of Ukraine
31 Nauky Prospect, Kyiv 03028, Ukraine*
[2]*Institute of Physics of National Academy of Sciences of Ukraine
46 Nauky Prospect, Kyiv 03028, Ukraine*
[3]*Research Center "ALT-Ukraine LTD"
4 Lunacharskiy Street, Kyiv 02002, Ukraine*

Photocatalytic NaAuCl$_4$ reduction by ethanol with the participation of ZnO nanocrystals results in the formation of gold nanocrystals with the mean size of 25–30 nm. The strongly pronounced autocatalytic character of the process reflects the fact that the ZnO–Au nanostructure produced at the initial stage of the photoreaction is a much more efficient photocatalyst than the original ZnO nanocrystals. The charging of gold nanocrystals by photogenerated ZnO conduction band electrons is accompanied by the equilibration of Fermi energies of the metal and semiconductor resulting in the charge redistribution between the components of ZnO–Au nanostructure and photoinduced polarization of ZnO nanocrystals. A long lifetime of the charged state of ZnO–Au nanostructure reflects an exceptional capability of gold nanocrystals to accumulate and retain negative charge.

INTRODUCTION

Modification of photoactive micro- and nanocrystalline semiconductors (TiO$_2$, ZnO, CdS, ZnS, etc.) with metal nanocrystals (NCs) is a powerful tool of enhancing efficiency and selectivity of the photocatalytic processes mediated by these semiconductor materials [1, 2]. The catalytic action of metal NCs originates either from the acceleration of interfacial conduction band electron (e^-_{CB}) transfer from a semiconductor to a substrate of the photoreaction as, for example, in case of TiO$_2$/Pt [1] or ZnO/Pt [3, 4] nanostructures, or in accumulation and retaining of negative charge (TiO$_2$/Au [1, 5, 6], ZnO–Au [4], ZnO/Ag [3], etc.). The latter factor favors to the redox-processes requiring a high potential barrier to be overcome and interferes to some extent with the electron-hole recombination in the semiconductor.

Among the metal-semiconductor nanostructures, of special interest are those incorporating gold NCs such as TiO$_2$/Au [7–11] and ZnO–Au [12–18] which possess unique charging capacity due to various chemical, photo- and electrochemical electron injection processes. These nanostructures find applications as redox photocatalysts [1, 2, 5, 6] and optical sensors [11, 15], in data storage systems [8, 9, 19] and non-linear optical media [12] as well as substrates for the surface-enhanced Raman spectroscopy [15, 16].

The metal-semiconductor nanostructures based on gold NCs are usually synthesized by the electrostatic binding of separately prepared metal and semiconductor NCs (ZnO–Au [4, 16, 18], TiO$_2$/Au [5, 6, 9]), by deposition of a layer or separate NCs of gold onto the semiconductor surface at the thermal reduction of gold(I, III) compounds (ZnO–Au [15, 17], TiO$_2$/Au [7, 8, 20], ZrO$_2$/Au [7]) or vice versa by the deposition of semiconductor nanoparticles onto gold NCs (Au/CdS [21, 22], Au/ZnO [13, 14]).

To prepare the metal-semiconductor nanostructures with advanced photocatalytic properties. a photochemical approach is widely used employing the photocatalytic reduction of metal compounds with the participation and on the surface of photoactive semiconductors − TiO$_2$, ZnO, CdS, ZnS, etc. [19]. In regard to the gold-based nanostructures, this approach was applied to synthesize ZnS/Au [24] and TiO$_2$/Au nanostructures [10,

* Corresponding author *stroyuk@inphyschem-nas.kiev.ua*

11] as well as to change the size of gold NCs in TiO$_2$/Au nanocomposites [8, 9].

At the same time, the photocatalytic reduction of gold compounds with the participation of nanocrystalline zinc oxide, the formation and properties of ZnO–Au nanostructures have not yet become a subject of a detailed investigation. In this connection, we report on the photocatalytic reduction of NaAuCl$_4$ by ethanol with the participation of colloidal ZnO NCs under UV light illumination. The photoprocess was shown to have distinct autocatalytic character and produce gold NCs with the average size of 25–30 nm. The photo-produced ZnO–Au nanostructures show the capability of photoinduced charging with electrons under stationary illumination even in the presence of molecular oxygen.

EXPERIMENTAL

Colloidal ZnO solutions in dry ethanol were synthesized from zinc acetate and NaOH and aged for 2 h at 55–60°C [25]. The average size of ZnO NCs was varied by changing the concentration of reactants in the range of 2×10^{-3}–2×10^{-2} M.

Illumination of colloidal solutions was carried out in the glass 10.0 mm optical cuvettes by the high-pressure 1000 W mercury lamp in a narrow spectral window of $\lambda = 310$–370 nm where the light intensity was $I_0 = 1.6\times10^{18}$ quanta per min.

Absorption spectra were recorded with a Specord 210 spectrophotometer. Transmission electron microscopy (TEM) data were obtained with a Selmi PEM-125K (Ukraine) with the accelerating voltage of 100 kV. X-Ray patterns were registered on a URS-002 setup using copper K_α irradiation. Dynamic light scattering spectra were obtained using a Malvern Zetasizer Nano S at 25°C. Solutions were illuminated by a He-Ne laser at $\lambda = 633$ nm, the scattered light registered at an angle of 173°.

RESULTS AND DISCUSSION

Illumination of a colloidal ZnO solution containing NaAuCl$_4$ results in the extinction of the absorbance of gold complex with the threshold at 450 nm (Fig. 1, curve *1*) and simultaneous rising of a new band at 500–650 nm with a maximum at 535–575 nm (Fig. 1, curves *2–9*). The new band corresponds to the surface plasmon resonance (SPR) in gold NCs [26–31] indicating that the

photoreduction of Au^{III} complex and formation of Au NCs take place in the system under examination. This reaction is of the photocatalytic nature because it requires both the illumination and the presence of ZnO NCs.
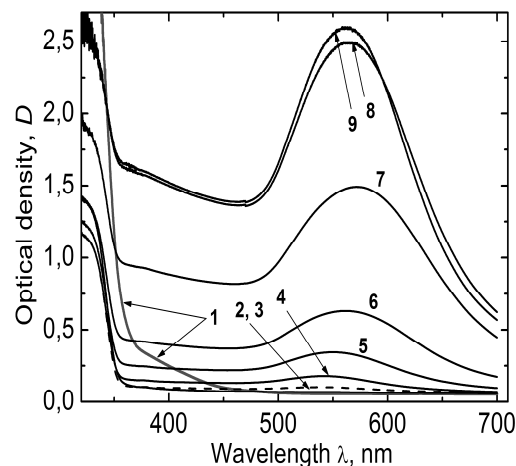

Fig. 1. The absorption spectra of a colloidal ZnO solution containing NaAuCl$_4$ before (*curve 1*) and after the illumination during 30 (*2*), 60 (*3*), 90 (*4*), 120 (*5*), 150 (*6*), 210 (*7*), 300 (*8*), and 360 s (*9*); [ZnO] = 2×10^{-3} M, [NaAuCl$_4$] = 5×10^{-4} M

The photoinduced formation of gold NCs is further confirmed by the examination of a Debye pattern of the photoproduct obtained after the solvent evaporation and soluble salts removal (Fig. 2*a*). The presented XRD photograph has patterns typical of both the hexagonal zinc oxide (labeled by indices on the figure) [32, 33] and the face-centered cubic gold [34].

According to TEM results (Fig. 2*b*), the photocatalytic NaAuCl$_4$ reduction with the participation of ZnO NCs produces gold NCs with a quite wide size distribution (10–60 nm) and the mean size of 25–30 nm (Fig. 2*c*).

A volume-normalized dynamic light scattering spectrum presented in Fig. 2*d* reveals the presence of two sorts of particles in the solution after the photocatalytic process is finished − the main fraction of relatively small 4.5 nm particles and the secondary one of larger particles with the average size of 30 nm (Fig. 2*d*).

The size of the first particle group correlates well with the average size of ZnO NCs calculated from the position of the absorption band edge in terms of a semi-empirical model presented in [35]. This result of the model, in contrast
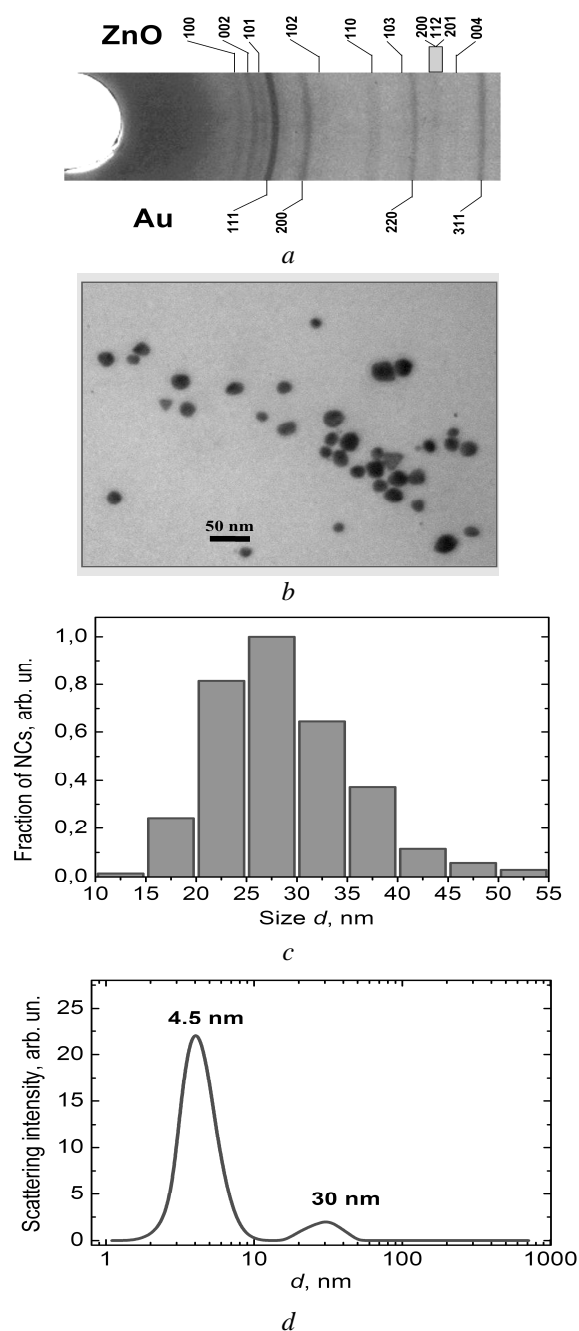
a

b

c

d

Fig. 2. (*a*) Debye diffraction photograph of the product of photocatalytic NaAuCl$_4$ reduction with the participation of ZnO NCs. (*b*) A TEM photograph of Au NCs produced by the photocatalytic reduction of NaAuCl$_4$ over ZnO NCs. (*c*) The size distribution of the photoproduced Au NCs derived from the TEM results (230 measurements of separate NCs). (*d*) Size distribution plot based on the results of dynamic light scattering spectroscopy of a colloidal ZnO/Au solution. The solution was prepared due to illumination of a ZnO colloid (1×10^{-3} M) in the presence of NaAuCl$_4$ (2.5×10^{-4} M)

to the effective mass approximation, agrees well with the reported experimental results on the relationship between the size d and the band gap E_g of ZnO NCs obtained by TEM and XRD [36, 37]. For E_g = 3.48 eV this model gives d = 4.4 nm.

In view of the above-discussed TEM data (Fig. *2b,c*), the second peak around 30 nm can be attributed to the photocatalytically produced Au NCs.

Fig. *3a* shows that the photocatalytic reduction of NaAuCl$_4$ mediated by ZnO NCs has a pronounced autocatalytic character. The photoprocess, though being slow during the first 100 s, gradually accelerates (100–200 s) and at t > 200 s stops with the entire present gold complex quantitatively reduced to Au^0. Some increase in gold concentration is also observed in the dark after initial 100 s exposure of the solution to the photoexcitation. As shown below, this fact can be explained by the photoinduced charging of gold NCs rather than by their catalytic properties.

The presented results indicate that the ZnO–Au nanostructure generated at the initial stage of photoreaction is a much more active photocatalyst of NaAuCl$_4$ reduction than original ZnO NCs. This is why, further photoreduction of Au^{III} complex would take place almost exclusively on the surface of gold NCs contacting with the ZnO NCs. The advanced photocatalytic properties of ZnO–Au nanostructures in the reaction under study can be associated with the well-known capability of gold NCs to accept conduction band electrons of zinc oxide NCs and to accumulate a negative charge [4, 8, 10, 26, 28] which can substantially promote three-electron reduction of NaAuCl$_4$ to Au^0.

The conditions of photochemical experiments were chosen so that the light absorption by colloidal solutions was incomplete, thus allowing all the present ZnO NCs to be photoexcited and to participate in the photocatalytic reaction. Under such conditions a uniform distribution of gold among the ZnO NCs and formation of Au NCs equal in size to the photocatalyst NCs can be expected. Nevertheless, these assumptions do not agree with the results of TEM and dynamic light scattering spectroscopy.

The formation of a small number of relatively large Au NCs can not be explained only by the agglomeration of smaller NCs. It can be seen from the XRD photograph (Fig. *2a*) that

the gold-related bands are not substantially broadened, as can be expected for NCs smaller than 10 nm. The TEM image of the photoproduct also shows no signs of the Au NC agglomeration. On the contrary, isolated gold NCs with a well-defined polyhedral shape can be seen in Fig. 2*b*.

In principle, one can assume that only a part of ZnO NCs gets involved into the photocatalytic process, for example, a fraction of smaller NCs with more pronounced photochemical activity. This assumption, however, is not supported by the experimental results which showed the photoprocess rate to be invariable with the decrease in the mean size of ZnO NCs from 4.4 to 3.7 nm.

Considering the above discussion, the photocatalytic formation of gold NCs, which are larger than the photocatalyst NCs themselves, can be interpreted in terms of simultaneous reactions of $AuCl_4^-$ reduction by photogenerated conduction band electrons and oxidation of ultrafine Au NCs by valence band holes or dissolved oxygen. For example, oxidation of photodeposited gold by valence band holes in the similar system based on ZnS NCs and $KAu(CN)_2$, facilitated by the presence of released cyanide ions, results in the equilibrium character of the photocatalytic formation of Au NCs [23, 24]. In the system containing ZnO NCs and $KAu(CN)_2$ the gold reduction is not observed at all what can be accounted for by a higher valence band potential of zinc oxide ($E_{VB} > 2.5$ eV [3]) as compared to ZnS NCs ($E_{VB} = 1.6–1.7$ eV [23, 24]).

The oxidation of gold by the valence band holes of TiO_2 NCs results in the enlargement of Au NCs [8]. The driving force of this process lies probably in the oxidation of a fraction of smaller gold NCs to Au^{III} by the photogenerated holes followed by the reduction of Au^{III} to Au^0 by the conduction band electrons and redeposition of gold on the surface of larger Au NCs [8]. Similar process can take place in the system under study. It should be noted that here not only the valence band holes of ZnO NCs but also molecular oxygen can act as an oxidizer of primary gold NCs.

The position of SPR band maximum (λ_{max}) of growing Au NCs undergoes a complex change in the course of photocatalytic reaction (Fig. 3*b*). It is well known that the SPR maximum of 10–30 nm gold NCs in ethanol pre-

pared without additional (photo)catalysts by $AuCl_4^-$ reduction is positioned at $\lambda_{max} \approx 520$ nm [26–31]. The maximum of SPR band of the product of photocatalytic $AuCl_4^-$ reduction with the participation of ZnO NCs appears at 537 nm at the beginning of the photoprocess and shifts in the course of illumination to longer wavelengths. The "red" shift of λ_{max} develops in the first 200 s of illumination, that is, in a period of fast $NaAuCl_4$ transformation (see Fig. 3*a*). At $t > 200$ s the shift of λ_{max} becomes slower and then reverses its direction to shorter wavelengths.
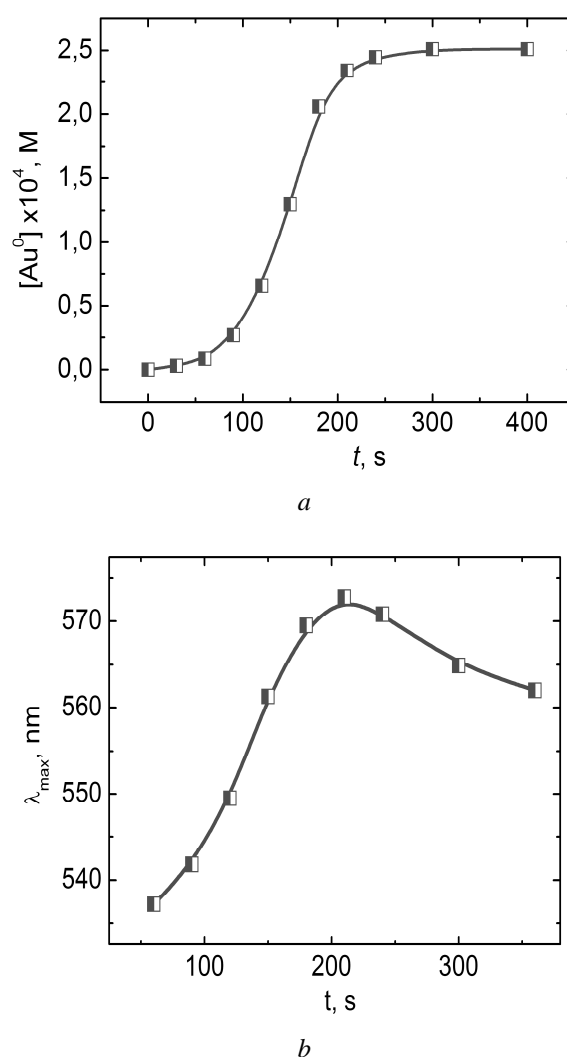

Fig. 3. (*a*) Kinetic curve of the photocatalytic formation of metal gold in the air-saturated colloidal ZnO solution. (*b*) The variation of the SPR band maximum position (λ_{max}) in the course of the photocatalytic $NaAuCl_4$ reduction. [ZnO] = 2×10^{3} M, [$NaAuCl_4$] = 5×10^{-4} M

_____

The position of SPR band maximum is determined mainly by the dielectric constant of a solvent and the density of free electrons N_e [26, 28]

$$\lambda_{max}^2 = \frac{(2\pi c)^2 m_e (\varepsilon_0 + 2n_0^2)}{4\pi e^2 N_e},$$

where c is the light velocity in vacuum, m_e and e are the rest mass and charge of electron, ε_0 is a wavelength-independent component of the dielectric constant of metal, and n_0 is the refractive index of the solvent.

A "red" shift of gold SPR band maximum produced in the photocatalytic reaction in the presence of ZnO NCs, as compared to λ_{max} of Au colloids in ethanol prepared without catalysts (520 nm), is typical of gold-semiconductor nanostructures both with the "core-shell" structure [13, 14, 21] and formed by separate contacting metal and semiconductor NCs [4, 7, 10–12, 17]. For example, the TiO_2/Au nanostructures show the SPR band maximum at 535–560 nm [7, 11], ZnO–Au – at 540–570 nm [12, 14], CdS/Au – at 540–555 nm [21, 22], ZnS/Au – at 550 nm [23, 24], and so on. The longer-wave shift of λ_{max} can be interpreted in terms of partial shielding of Au NCs by the semiconductors which have a higher refraction index than that of the solvent. This effect can be accounted for by using an effective value of n_0 in the expression averaging the effects of both the semiconductor and solvent upon the parameters of surface plasmon resonance of gold NCs.

According to [27, 29–31], the variation of λ_{max} with the size of Au NCs is rather small for the range of 10–30 nm and can therefore be neglected. Considering this fact, the reason for the long-wave λ_{max} shift of growing Au NCs can lie in a change of their surface state. At that, a possible factor may be the adsorption of ZnO NCs on the surface of gold NCs. As the size of Au NCs increases, the number of ZnO NCs adsorbed on the metal surface grows as well. This results in a more pronounced shielding of gold NCs from the solvent and an increase of the effective refractive index of dispersion medium. This factor can also make a certain contribution into the autocatalytic character of the photoprocess since it allows several ZnO NCs

to inject photogenerated electrons into the adjacent Au NC.

Another possible reason for the long-wave shift of λ_{max} in the course of illumination can lie in the extinction of $AuCl_4^-$ ions adsorbed on the surface of gold NCs. The adsorption of anions and neutral nucleophilic compounds on the surface of gold NCs is known to increase N_a in a near-surface NC layer shifting λ_{max} to shorter wavelengths [26, 28]. As the photocatalytic reaction proceeds, the $AuCl_4^-$ anions are consumed resulting in a decrease of N_a and the long-wave shift of the SPR band maximum.

After complete transformation of $NaAuCl_4$ is achieved and the Au NCs completely grown, the illumination of solutions results in a short-wave shift of λ_{max} (Fig. 3*b*). The fact can be accounted for by the charging of gold NCs with electrons accepted from ZnO NCs. In a similar TiO_2/Au^0 system this phenomenon is observed even in the presence of an efficient electron acceptor – O_2 [10], the fact reflecting an exceptional capability of Au NCs to accumulate and retain the negative charge [4, 22, 28].

On the final stage of the photoprocess the short-wave λ_{max} shift is accompanied by a short-wave shift of the absorption band edge of ZnO NCs. This observation indicates that ZnO NCs become charged as well [3, 4]. The excess electrons occupy states near the "bottom" of conduction band increasing in this way the energy of optical interband transition (the dynamic Burstein-Moss effect) [38, 39]. The charging of ZnO NCs indicates the Fermi level equilibration of the charged semiconductor and metal resulting in a partial redistribution of electrons between Au and ZnO NCs [3, 4]. When kept in the dark, both the absorption band edge of ZnO NCs and the SPR band maximum return to their long-wave positions indicating gradual discharge of ZnO–Au nanostructures (Fig. 4*a*).

Another evidence of the Au NCs charging during the photoreaction is the formation of an additional quantity of gold when keeping the previously illuminated for a short time solution in the dark (Fig. 4*b*).

It should be noted that exceptionally long (tens of hours) retention of the negative charge by the illuminated ZnO–Au nanostructures in the presence of oxygen distinguishes this system
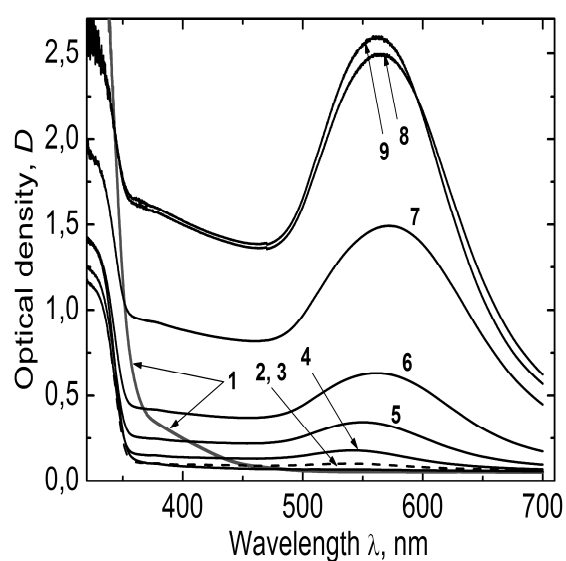
a
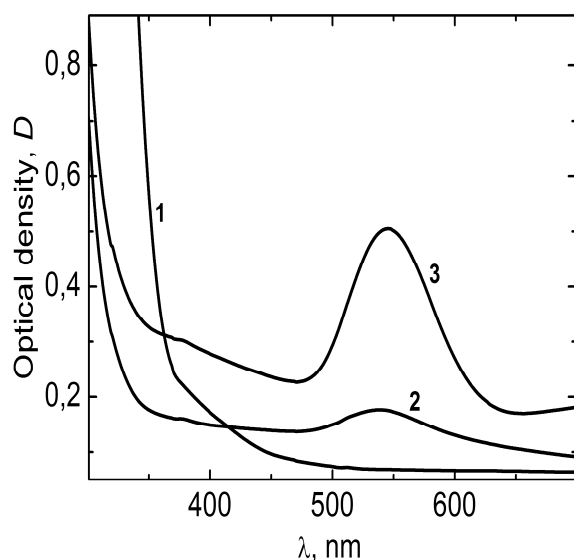
b

Fig. 4. (*a*) The absorption spectra of a colloidal ZnO/Au solution produced at illumination of ZnO colloid (1×10^{3} M) in the presence of NaAuCl$_4$ (2.5×10^{-4} M) during 4 min immediately after the photoprocess termination (*curve 1*) and after keeping the solution in the dark for 5 (*2*) and 15 h (*3*). Inset: a magnified section of the absorption spectra corresponding to the absorption band of ZnO NCs. (*b*) The absorption spectra of a colloidal ZnO solution (2.5×10^{4} M) containing 2.5×10^{-4} M NaAuCl$_4$ prior to (*curve 1*) and after 3 min illumination (*2*), as well as after keeping the illuminated solution in the dark for 17 h (*3*)

from its close analogues, such as ZnO/Ag [3, 40] and ZnO/Cu [3, 25] where the photoinduced charging effect is observed only in the deaerated solutions and disappears promptly after the air admission. The results discussed are apparently the first evidence of the prolonged photoinduced charging of ZnO NCs under the stationary illumination in the presence of molecular oxygen.

CONCLUSIONS

The photocatalytic NaAuCl$_4$ reduction with the participation of ZnO NCs results in the formation of nanometer gold crystals with the average size of 25–30 nm. The distinct autocatalytic character of the photoprocess indicates that the ZnO–Au produced have much higher photocatalytic activity in Au^{III} reduction as compared with the original zinc oxide NCs.

After the complete transformation of gold(III) complex the photoproduced Au NCs become charged by the photogenerated conduction band electrons of ZnO NCs. This process is accompanied by the equilibration of the Fermi levels of the metal and semiconductor and the photoinduced charging of ZnO NCs. The ZnO–Au nanostructure remains in the charged state for a long time (tens of hours) even in the presence of an efficient electron acceptor – molecular oxygen. The fact indicates an exceptional capability of gold NCs to accumulate and retain negative charge.

REFERENCES

1. Energy resources through photochemistry and catalysis / Ed. M. Grätzel. – N.-Y.: Academic Press, 1983. – 588 p.
2. *Stroyuk A.L., Kryukov A.I., Kuchmiy S.Ya., Pokhodenko V.D.* Quantum size effects in semiconductor photo catalysis // Theor. Exp. Chem. – 2005. – V. 41, N 4. – P. 207–228.
3. *Wood A., Giersig M., Mulvaney P.* Fermi level equilibration in quantum dot-metal nanojunctions // J. Phys. Chem. B. – 2001. – V. 105, N 37. – P. 8810–8815.
4. *Subramanian V., Wolf E.E., Kamat P.V.* Green emission to probe photoinduced charging events in ZnO–Au nanoparticles. Charge distribution and Fermi-level

_____

equilibration // J. Phys. Chem. B. – 2003. – V. 107, N 30. – P. 7479–7485.

5. *Subramanian V., Wolf E.E., Kamat P.V.* Semiconductor-metal composite nanostructures. To what extent do metal nanoparticles improve the photocatalytic activity of TiO₂ films? // J. Phys. Chem. B. – 2001. – V. 105, N 46. – P. 11439–11446.

6. *Subramanian V., Wolf E.E., Kamat P.V.* Influence of metal/metal ion concentration on the photocatalytic activity of TiO₂–Au composite nanoparticles // Langmuir. – 2003. – V. 19, N 2. – P. 469–474.

7. *Furube A., Du L., Hara K. et al.* Ultrafast plasmon-induced electron transfer from gold nanodots into TiO₂ nanoparticles // J. Amer. Chem. Soc. – 2007. – V. 129, N 48. – P. 14852–14853.

8. *Kawahara T., Soejima T., Mitsui T. et al.* Photoinduced dissolution and redeposition of Au nanoparticles supported on TiO₂ // J. Colloid Interface Sci. – 2005. – V. 286, N 2. – P. 816–819.

9. *Dolamic I., Gautier C., Boudon J. et al.* Adsorption of thiol-protected gold nanoparticles on TiO₂ and their behavior under UV light irradiation // J. Phys. Chem. C. – 2008. – V. 112, N 15. – P. 5816–5824.

10. *Soejima T., Tada H., Kawahara T., Ito S.* Formation of Au nanoclusters on TiO₂ surfaces by a two-step method consisting of Au(III)-complex chemisorption and its photoreduction // Langmuir. – 2002. – V. 18, N 11. – P. 4191–4194.

11. *Tanahashi I., Iwagishi H., Chang G.* Localized surface plasmon resonance sensing properties of photocatalytically prepared Au/TiO₂ films // Mater. Lett. – 2008. – V. 62, N 17–18. – P. 2714–2716.

12. *Ning T., Zhou Y., Shen H. et al.* Nonlinear optical properties of Au/ZnO nanoparticle arrays // Appl. Surf. Sci. – 2009. – V. 254, N 1–2. – P. 1900–1903.

13. *Lee M.-K., Kim T.G., Kim W., Sung Y.-M.* Surface plasmon resonance (SPR) electron and energy transfer in noble metal-zinc oxide composite nanocrystals // J. Phys. Chem. C. – 2008. – V. 112, N 27. – P. 10079–10082.

14. *Haldar K.K., Sen T., Patra A.* Au@ZnO core-shell nanoparticles are efficient energy acceptors with organic dye donors // J. Phys. Chem. C. – 2008. – V. 112, N 31. – P. 11650–11656.

15. *Shan G., Wang S., Fei X. et al.* Heterostructured ZnO/Au nanoparticles-based resonant Raman scattering for protein detection // J. Phys. Chem. B. – 2009. – V. 113, N 5. – P. 1468–1472.

16. *Yang L., Ruan W., Jiang X. et al.* Contribution of ZnO to charge-transfer induced surface-enhanced Raman scattering in Au/ZnO/PATP assembly // J. Phys. Chem. C. – 2009. – V. 113, N 1. – P. 117–120.

17. *Shan G., Zhong M., Wang S. et al.* The synthesis and optical properties of the heterostructured ZnO/Au nanocomposites // J. Colloid Interface Sci. – 2008. – V. 326, N 2. – P. 392–395.

18. *Chen B., Zhang H., Du N. et al.* Hybrid nanostructures of Au nanocrystals and ZnO nanorods: Layer-by-layer assembly and tunable blue-shift band gap emission // Mater. Res. Bull. – 2009. – V. 44, N 4. – P. 889–892.

19. *Stroyuk A.L., Shvalagin V.V., Raevskaya A.E. et al.* Photochemical formation of semiconductor nanostructures // Theor. Exp. Chem. – 2008. – V. 44, N 4. – P. 199–220.

20. *Kamat P.V., Shanghavi B.* Interparticle electron transfer in metal/semiconductor composites. Picosecond dynamics of CdS-capped gold nanoclusters // J. Phys. Chem. B. – 1997. – V. 101, N 39. – P. 7675–7679.

21. *Chen W.-T., Yang T.-T., Hsu Y.-J.* Au-CdS core-shell nanocrystals with controllable shell thickness and photoinduced charge separation property // Chem. Mater. – 2008. – V. 20, N 23. – P. 7204–7206.

22. *Sun L., Wei G., Song Y. et al.* Solution-phase synthesis of Au@ZnO core-shell composite // Mater. Lett. – 2006. – V. 60, N 9–10. – P. 1291–1295.

23. *Raevskaya A.E., Korzhak A.V., Stroyuk A.L., Kuchmiy S.Ya.* Phocatalysis by ZnS nanoparticles of the formation of

ZnS/Au heterostructure in the reduction of complex ions of gold // Theor. Exp. Chem. – 2005. – V. 41, N 6. – P. 359–364.

24. *Stroyuk A.L., Raevskaya A.E., Korzhak A.V., Kuchmiy S.Ya.* Zink sulfide nanoparticles: Spectral properties and photocatalytic activity in metals reduction reactions // J. Nanopart. Res. – 2007. – V. 9, N 6. – P. 1027–1039.

25. *Stroyuk A.L., Shvalagin V.V., Kuchmiy S.Ya.* Photochemical synthesis and optical properties of binary and ternary metal-semiconductor composites based on zinc oxide nanoparticles // J. Photochem. Photobiol. A. – 2005. – V. 173, N 2. – P. 185–194.

26. *Henglein A.* Physicochemical properties of small metal particles in solution: "microelectrode" reactions, chemisorption, composite metal particles, and the atom-to-metal transition // J. Phys. Chem. – 1993. – V. 97, N 21. – P. 5457–5471.

27. *Njoki P.N., Lim I-I. S., Mott D. et al.* Size correlation of optical and spectroscopic properties for gold nanoparticles // J. Phys. Chem. C. – 2007. – V. 111, N 40. – P. 14664–14669.

28. *Henglein A.* Radiolytic preparation of ultrafine colloidal gold particles in aqueous solution: Optical spectrum, controlled growth, and some chemical reactions // Langmuir. – 1999. – V. 15, N 20. – P. 6738–6744.

29. *Foss C.A., Hornyak G.I., Stockert J.A., Martin C.R.* Template-synthesized nanoscopic gold particles: Optical spectra and the effects of particle size and shape // J. Phys. Chem. – 1994. – V. 98, N 11. – P. 2963–2971.

30. *Link S., El-Sayed M.A.* Size and temperature dependence of the plasmon absorption of colloidal gold nanoparticles // J. Phys. Chem. B. – 1999. – V. 103, N 21. – P. 4212–4217.

31. *Seshadri R., Subbanna G.M., Vijayakrishnan V. et al.* Growth of nanometric gold particles in solution phase // J. Phys. Chem. – 1995. – V. 99, N 15. – P. 5639–5644.

32. *Audebrand N., Auffrédic J.-P., Louër D.* X-ray diffraction study of the early stages of the growth of nanoscale zinc oxide crystallites obtained from thermal decomposition of four precursors. General concepts on precursor-dependent microstructural properties // Chem. Mater. – 1998. – V. 10, N 9. – P. 2450–2461.

33. *Guo L., Yang S.* Synthesis and characterization of poly (vinylpyrrolidone)-modified zinc oxide nanoparticles // Chem. Mater. – 2000. – V. 12, N 8. – P. 2268–2274.

34. *Leff D.V., Ohara P.C., Heath J.R., Gelbart W.M.* Thermodynamic control of gold nanocrystal size: Experiment and theory // J. Phys. Chem. – 1995. – V. 99, N 18. – P. 7036–7041.

35. *Fonoberov V.A., Balandin A.A.* Radiative lifetime of excitons in ZnO nanocrystals: The dead-layer effect // Phys. Rev. B. – 2004. – V. 70, N 1. – P. 195410 (1–5).

36. *Wood A., Giersig M., Hilgendorff M. et al.* Size Effects in ZnO: The Cluster to Quantum Dot Transition // Aust. J. Chem. – 2003. – V. 56, N 10. – P. 1051–1057.

37. *Wang Y.S., Thomas P.J., O`Brien P.* Nanocrystalline ZnO with ultraviolet luminescence // J. Phys. Chem. B. 2006. – V. 110, N 9. – P. 4099–4104.

38. *Liu C.Y., Bard A.J.* Effect of excess charge on band energetics (optical absorption edge and carrier redox potentials) in small semiconductor particles // J. Phys. Chem. – 1989. – V. 93, N 8. – P. 3232–3237.

39. *Kamat P.V., Dimitrijevic N.M., Nozik A.J.* Dynamic Burstein-Moss shift in semiconductor colloids // J. Phys. Chem. – 1989. – V. 93, N 8. – P. 2873–2875.

40. *Shvalagin V.V., Stroyuk A.L., Kuchmiy S.Ya.* Photochemical synthesis of ZnO/Ag nanocomposites // J. Nanopart. Res. – 2007. – V. 9, N 3. – P. 427–440.

Фотокаталітичне утворення та фотоіндуковане зарядження наноструктур ZnO–Au

О.Л. Строюк, **В.В. Швалагін** , **І.Є. Котенко**, **С.Я. Кучмій**, **А.Г. Держипольський**, **Д.А. Меленевський**

Інститут фізичної хімії ім. Л.В. Писаржевського Національної академії наук України
пр. Науки 31, Київ 03028, Україна, stroyuk@inphyschem-nas.kiev.ua
Інститут фізики Національної академії наук України
пр. Науки 46, Київ 03028, Україна
Дослідницький центр ТОВ"АЛТ-Україна ЛТД"
вул. Луначарського 4, Київ 02002, Україна

Фотокаталітичне відновлення NaAuCl₄ етанолом за участю нанокристалів ZnO приводить до утворення наночастинок золота з середнім розміром 25–30 нм. Яскраво виражений аутокаталітичний характер фотопроцесу свідчить про те, що наногетероструктури ZnO–Au, які формуються на початковому етапі реакції, є набагато ефективнішим фотокаталізатором, аніж вихідні нанокристали оксиду цинку. Зарядження нанокристалів золота електронами, фотогенерованими у зоні провідності ZnO, супроводжується вирівнюванням рівнів Фермі металу та напівпровідника, перерозподілом зарядів між компонентами наногетероструктури ZnO–Au та фотоіндукованою поляризацією нанокристалів ZnO. Тривале збереження зарядженого стану наноструктури ZnO–Au свідчить про виняткову здатність нанокристалів золота до накопичення та утримування негативного заряду.

Фотокаталитическое получение и фотоиндуцированная зарядка наноструктур ZnO–Au

А.Л. Строюк, В.В. Швалагин, И.Е. Котенко, С.Я. Кучмий, А.Г. Держипольский, Д.А. Меленевский

Институт физической химии им. Л.В. Писаржевского Национальной академии наук Украины
пр. Науки 31, Киев 03028, Украина, stroyuk@inphyschem-nas.kiev.ua
Институт физики Национальной академии наук Украины
пр. Науки 46, Киев 03028, Украина
Исследовательский центр ООО"АЛТ-Украина ЛТД"
ул. Луначарского 4, Киев 02002, Украина

Фотокаталитическое восстановление NaAuCl₄ этанолом при участии нанокристаллов ZnO приводит к формированию наночастиц золота со средним размером 25–30 нм. Ярко выраженный автокаталитический характер фотопроцесса свидетельствует о том, что формирующиеся на начальном этапе реакции наногетероструктуры ZnO–Au являются гораздо более активным фотокатализатором, чем исходные нанокристаллы оксида цинка. Зарядка нанокристаллов золота электронами, фотогенерированными в зоне проводимости ZnO, сопровождается выравниванием уровней Ферми металла и полупроводника, перераспределением заряда между компонентами наногетероструктуры ZnO–Au и фотоиндуцированной поляризацией нанокристаллов ZnO. Длительное пребывание наноструктур ZnO–Au в заряженном состоянии свидетельствует об исключительной способности нанокристаллов золота к аккумулированию и удерживанию отрицательного заряда.